Wood Science & Technology, in press (2014) (DOI: 10.1007/s00226-014-0661-0)

Measuring Interfacial Stiffness of Adhesively-Bonded Wood

Edward A. Le
University of Washington, Department of Mechanical Engineering, Seattle, WA 98195, USA
and National Cheng Kung University, Medical Device Innovations Center, Tainan,Taiwan

John A. Nairn
Wood Science & Engineering, Oregon State University, Corvallis, OR 97330, USA

Abstract

Adhesive bond line stiffness is an important property that plays a significant role in the properties of wood composites, but is typically ignored by methods used for characterizing adhesive quality. This paper proposes a new test method that can measure an *effective* bond line stiffness. The experiments measured the global stiffness of double lap shear specimens and then calculated an adhesive stiffness property using shear-lag analysis of each specimen's specific geometry and layer properties. Experiments were done for phenol formaldehyde (PF) and polyvinyl acetate (PVA) bonding wood strands of hybrid poplar and densified hybrid poplar. The stiffness of PF bond lines was an order of magnitude higher than PVA bond lines and both were affected by the amount of adhesive coverage. The bond line stiffness with densified wood was similar to, or higher than undensified wood despite the lack of penetration of resin into the densified strands.

1. Introduction

Adhesive bonds in wood composites have two roles. The first is to hold elements of the composite together. This role can be characterized as bond "strength." If the adhesive bond has insufficient strength, the interfaces will fail, the elements will cease to share load, and the composite will have poor properties. The second role, even in the absence of failure, is to transfer stress across the bond line between the bonded wood elements. This role can be characterized as bond "stiffness." A better (or "stiffer" interface) will transfer stress faster between elements and therefore result is superior composite stiffness properties. A "soft" adhesive bond (*e.g.*, one with insufficient adhesive) will result in slower stress transfer and reduced mechanical properties. Both bond strength and stiffness are important to the properties of adhesively bonded wood, including adhesive bonds in wood composites. The main role of bond strength is in ultimate

failure properties of the wood composite. Once strength achieves a sufficient level, however, the remaining composite properties are more determined by bond stiffness then by bond strength. In other words, strength is necessary for good wood composites but is not sufficient for most properties. For properties like modulus or thermal and moisture expansion coefficients, bond stiffness is the more important property.

Nearly all methods for characterizing wood adhesive bonds consider only strength of the bonds. Typically a bond line is loaded until failure and the final load at failure is recorded. Some common strength tests are lap shear testing (ASTM 2008a), shear block testing (ASTM 2008b), and internal bond testing (ASTM 2008c). Adhesive bonds are tested for fracture toughness (Kutnar, Kamke, and Sernek, 2008; ASTM 2005; ASTM E2006), but these are also probing failure properties of adhesive bonds. None of these adhesive tests monitor what happens prior to failure, but, as discussed above, what happens during that stage plays a major role in quality of the bond. For example, in a wood composite such as oriented strand board, it is unlikely that ordinary use is causing a large accumulation of adhesive failures. In these situations, it is "stiffness" of the glue line that would have the more practical relevance to product performance (Nairn and Le, 2009). Glue line stiffness will affect panel stiffness and therefore suitability of panels for various applications. Bond "strength" is largely irrelevant, except as a crude indicator of adhesion problems. We suggest that adhesion tests that characterize overall bond stiffness are as important, or more important, than current strength or fracture tests.

Another issue with adhesive bonds lines in wood is penetration of resin into wood cells. A common belief is that penetration is essential for good bonds because it leads to mechanical interlocking. This macroscopic view of a microscopic phenomenon may not be appropriate. More likely, there is an optimum amount of penetration. Determination of this optimum level requires characterization methods that measure both strength and stiffness of adhesive bonds. The role of penetration in bond strength is uncertain, except that if the bond line is starved of adhesive, strength will eventually suffer. The role of penetration in bond stiffness is that it creates an interphase zone where penetrated resin may modify local mechanical properties of the wood. This interphase zone will influence stress transfer, which translates to a change in overall stiffness of the bond line. Experiments aimed at bond stiffness are needed to investigate this effect.

This paper describes a new experimental protocol for measuring bond stiffness properties for adhesive bonds between wood strands. The test method is based on a standard double lap shear (DLS) test specimen (ASTM 2008d), but the experiments focus on specimen response prior to failure. Specifically, the experiments measure global stiffness of DLS specimens. To interpret these results, a shear lag model was developed that can calculate bond stiffness from the global stiffness assuming the mechanical properties and thicknesses of all layers are known. We

measured those properties in separate experiments prior to making the DLS specimens. This new bond-line test method was applied to wood strands glued by either phenol formaldehyde (PF) or polyvinyl acetate (PVA) resins. The amount of glue in the bond lines was varied to study role of adhesive coverage in stress transfer. To get some results about the effect of adhesive penetration, additional experiments were done on adhesively bonded, densified wood. The densification process limited penetration in those specimens.

2. Materials and Methods

The adhesive bonds studied were between wood strands typically found in oriented strand board (OSB) panels. Two types of strands were used. The first were strands cut from low-density, hybrid poplar wood (*Populus deltoides* X *Populus trichocarpa*). The as-supplied strands were further cut into specimens 6 mm wide and 150 mm long with the grain direction aligned well with the long axis of the specimen. These strands had average thickness of 0.82 mm and a density of 0.35 g/cm^3. To assess the role of adhesive penetration into wood cells, the second strands where thicker hybrid poplar strands that were processed by viscoelastic thermal compression (VTC) into higher density strands (Kutnar, Kamke, and Sernek, 2008). After VTC processing, the thickness was reduced from close to 3 mm to an average of 1.1 mm and the density increased to 0.93 g/cm^3. As with normal strands, these strands were cut into 6 mm by 150 mm specimens with the grain direction along the long axis of the specimens. Prior to testing, all strands were conditioned to 12% moisture content in a 20˚C, 65% relative humidity, conditioning room.

Two resins were used in this work. The first was a typical commercial phenol-formaldehyde (PF) resin used in OSB, and manufactured by Georgia Pacific Resins, Inc. The second was a polyvinyl acetate (PVA) resin, which is a typical wood glue manufactured by Tite Bond. The moduli these pure resins are difficult to quantify (especially for PF), but likely in the range of 1 to 2 GPa (López-Suevos 2010).

All interfacial mechanical tests were done on double lap shear (DLS) specimens (see Fig. 1). To be able to extract interfacial properties from DLS specimen results, it was essential to know the mechanical properties of each layer in the specimen. Because of variability in modulus of strands, we nondestructively measured the modulus of each individual strand prior to fabrication of the DLS specimens. As explained below, the analysis is simplified if the specimens are symmetric in both geometry and mechanical properties. To obtain this symmetry, one strand was cut in half and used for the two outer strands while a different strand was used for the center strand.

Once strands where selected and characterized, they were glued together into DLS specimens using a modified flexographic printing technique described by Smith (2003a, b):

1. The adhesive was spread on a glass plate using a wire-wrapped rod made by RD Specialties (Webster, New York, USA). The ½ in diameter rod was wrapped with 1 mm wire. This method produces a uniform adhesive layer on the glass plate (Smith 2003b).
2. Printing stamps were used to transfer adhesive from the glass plate to the specimens. The stamps were fabricated with surface textures consisting of circular dots of various diameters in a square array (by A-Z Stamps, Portland, OR, USA). The coverage obtained by a given stamp was controlled by varying the diameter of the dots and the number of dots per inch (Smith 2003b). The two printing stamps used in this study had surface coverage of 1% and 25%; these percentages refer to the fraction of the stamp surface with dots and not to the final amount of glue that ends up on the strands. The two different stamps, however, did provide reproducible, different, and incomplete adhesive coverage on the bond lines. Specimens with 100% coverage were made by manually spreading glue over entire surface.

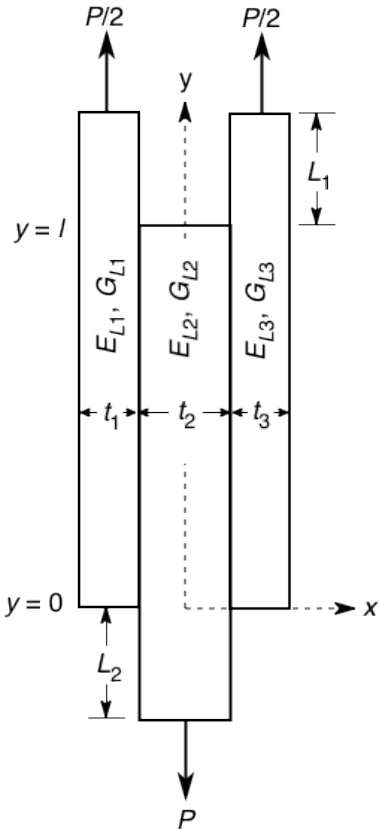

Figure 1: The double lap shear (DLS) specimen geometry. Each layer has its own moduli (E_{Li} and G_{Li}) and thickness (t_i). The bonded section is of length l. The unbonded ends of lengths L_1 and L_2 are distance from the end of the bonded section to the detection position for the extensometer.

3. The DLS specimens were assembled with a total bond length of 25 mm and then cured in a hot press at 0.689 MPa (100 psi) and 180˚C for 5 minutes.
4. After curing, the DLS specimens were reconditioned at 20˚C and 65% relative humidity for several days prior to testing.

2.1 Interfacial Stiffness Experiments

The effective stiffness of the bond line was measured by an inverse method, which means we measured global stiffness of DLS specimens and then back-calculated glue-line stiffness using a micromechanics model that incorporates an imperfect interfacial bond. Each specimen's global stiffness was measured in tension in an Instron model 5582 at 0.3 mm/min. The displacement

was measured with an extensometer having a gage length of 50 mm such that it spanned the entire bonded region of the specimen. Global stiffness was determined from the slope of force *vs*. extensometer displacement. This specimen stiffness is denoted here as k (in N/mm).

Calculation of interfacial properties from experimental k requires a micromechanics model. Figure 1 shows a double lap shear specimen where each layer may have a different longitudinal modulus (E_{Li}), longitudinal shear modulus (G_{Li}), and thickness (t_i). This specimen can be accurately modeled by shear-lag analysis that includes interfacial stiffness effects (Nairn 2004, 2007). In this model, interfacial stiffness was modeled using Hashin's (1990) model for imperfect interfaces in composites. In brief, all complexities of a 3D interphase region (*e.g.*, a zone of resin penetration), are collapsed to a 2D interface. The 2D interface is then allowed to develop discontinuities in displacement. The simplest model is to assume the displacement discontinuities are linear in traction forces in the same direction. For example, the axial displacement discontinuity between two strands in a DLS specimen, denoted with square brackets or $[w]$, is assumed to be proportional to interfacial shear stress, τ, or

$$[w] = \frac{\tau}{D_s} \tag{1}$$

where D_s is an interfacial stiffness parameter. As D_s approaches infinity, $[w]$ approaches zero and the bond is said to act as a "perfect" bond. As D_s approaches zero (and is moved to the other side of the equation), τ approaches zero and the interface is failed or debonded. All other values of D_s describe an imperfect interface as a model for a bond-line interphase zone. For a physical interpretation of D_s, one can imagine a physical interfacial layer of thickness, t_a, of pure adhesive with shear modulus, G_a, loaded by simple shear. In this simple geometry, the shear strain would be $\gamma = \tau/G_a = [w]/t_a$, which allows interpretation of D_s as equal to an effective G_a/t_a for the interfacial region.

This imperfect interface model was developed for compliant interfaces (Hashin 1990). In wood bonds, it is possible that resin penetration will reinforce the interphase zone resulting in a region that is stiffer than the adherends. This effect can be modeled in the same theory be allowing $1/D_s$ to pass through zero (the "perfect" bond condition) into negative values (Nairn 2007). Such negative interface parameters are energetically permissible provided $1/D_s$ is greater than a negative limit that would correspond to a rigid (or infinitely stiff) interphase zone; this rigid limit is easily determined by shear lag analysis. The Hashin (1990) approach is not claiming these complex interphases are 2D structures. Rather, by collapsing 3D details to a 2D mathematical model it reduces the number of unknown properties involving geometry and position-dependent properties of adhesive bond lines to a small number of interface parameters like D_s. In fact, for DLS specimens, D_s is the only interface parameter that is needed. The experiments described here were aimed at measuring D_s.

Although a full analysis with three different layers is possible, the equations are greatly simplified if the specimen is symmetric (*i.e.*, $E_{L1} = E_{L3}$, $G_{L1} = G_{L3}$, and $t_1 = t_3$); as explained above all specimens tested were made symmetric by using the same strand for the two outer layers. The global stiffness of a symmetric DLS specimen, which accounts for displacements in the unbonded ends (of length L_i), is

$$k = \frac{t_2 E_{L2} W}{\frac{C}{C_\infty}\frac{l}{1+2R\lambda} + \frac{L_1}{2R\lambda} + L_2} \tag{2}$$

where W is specimen width, $R = E_{L1}/E_{L2}$, $\lambda = t_1/t_2$, and thickness and end length dimensions are illustrated in Fig. 1. The ratio C/C_∞ is the ratio of the compliance of the bonded section (of length l) of the specimen relative to the compliance where the three strands deform as a unit with equal and constant strain throughout ($C_\infty = l/[(1+2R\lambda)t_2 E_{L2} W]$). This ratio can be found from shear-lag analysis (Nairn 2007):

$$\frac{C}{C_\infty} = 1 + \frac{(1-2R\lambda)^2 \tanh\frac{\beta l}{2} + (1+2R\lambda)^2 \tanh\frac{\beta l}{4}}{4\beta l R\lambda} + \frac{t_2 E_{L2}\beta(1+2R\lambda)}{4lD_s}\operatorname{csch}\frac{\beta l}{2} \tag{3}$$

The term β is the shear lag parameter, which in modern shear lag theory can account for glue line stiffness using the Hashin (1990) imperfect interface model (Nairn 2004, 2007A):

$$\beta^2 = \frac{\frac{1}{t_1 E_{L1}} + \frac{2}{t_2 E_{L2}}}{\frac{t_1}{3G_{L1}} + \frac{t_2}{6G_{L2}} + \frac{1}{D_s}} \tag{4}$$

Nairn (2007) gave C/C_∞ for three identical layers. Equation (3) extends that result to symmetric specimens where the center layer is different; it reduces to the result in Nairn (2007) for the special case or $R = \lambda = 1$. The rigid limit for allowable negative D_s values is when the denominator in Eq. (4) is zero; in other words, the permissible range for D_s requires:

$$\frac{1}{D_s} > -\left(\frac{t_1}{3G_{L1}} + \frac{t_2}{3G_{L2}}\right) \tag{4}$$

Approximate models, such as the above shear-lag analysis, should not be used unless they are first verified as accurate. To verify shear-lag micromechanics for a DLS specimen, the predictions were compared to finite element analysis (FEA) with Hashin, imperfect interface elements between the strands (Nairn 2007). The results are in Fig. 2 and were done for three identical strands with E_{Li} = 7500 MPa, G_{Li} = 500 MPa, t_i = 0.7 mm, l = 25 mm, W = 10 mm, and L_i = 5 mm. The shear-lag analysis (solid lines) agrees well with FEA results (symbols)

By equations (2), (3), and (4), the measured k is a function of E_{L1}, G_{L1}, E_{L2}, G_{L2}, and D_s as well as geometric variables t_1, t_2, l, W, L_1, and L_2. In these experiments, we measured all geometric variables for each DLS specimen and measure E_{L1} and E_{L2} for each strand. The moduli

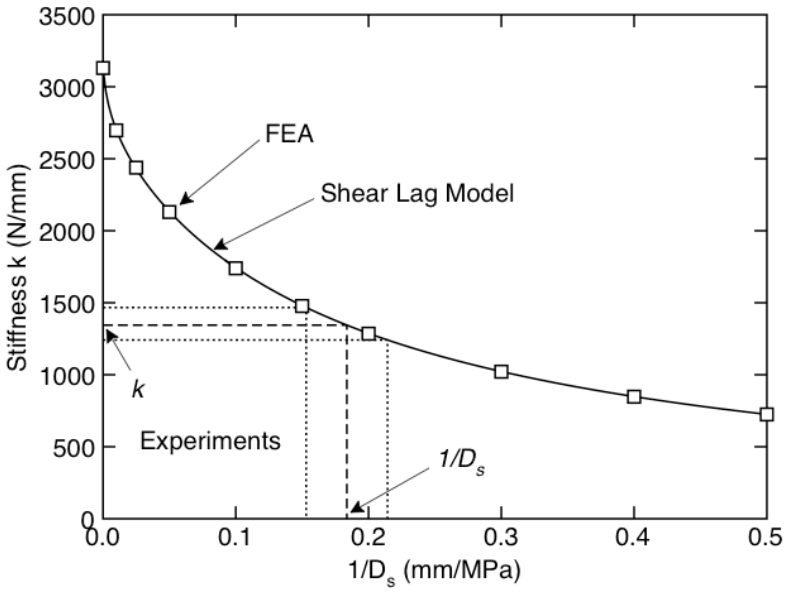

Figure 2: Comparison of shear lag model with an imperfect interface (i.e., Eqs. (2) to (4)) to finite element calculations (FEA) using imperfect interface elements (symbols). The horizontal and vertical lines labeled "Experiments" graphically demonstrate the analysis process and the method for determining uncertainty.

were found by testing 6 mm X 150 mm strand specimens nondestructively in an Instron model 5582 with displacement measured using a clip-gage extensometer. More than 1000 specimens were tested. We estimated G_{L1} and G_{L2} by typical ratios between tensile and shear moduli for wood ($G \approx E/15$). Finally, D_s remained as the only unknown. That property was determined by numerically solving Eq. (2) for D_s for each measured k; a Java application was written to do the calculations.

The numerical process for finding D_s is illustrated graphically by the dashed line in Fig. 2. A horizontal line is drawn from an experimentally determined k until it intersects the shear-lag k *vs*. $1/D_s$ curve for a specific specimen's properties calculated by Eq. (2). A vertical line drawn down from the intersection point gives an experimental result for D_s. The accuracy of these experiments depends on the k *vs*. $1/D_s$ curve. Ideally, the curve should vary rapidly with D_s within the range of experimental values for k. Eqs. (2) to (4) were used to choose specimen dimensions. The most important parameter is length of the bonded region (l). Most of the shear that induces interfacial slippage in DLS specimens (by Eq. (1)) occurs at the ends of the bonded region. If bond length gets too large, the role of that shear diminishes, as does the role of the interface in specimen k. In contrast, shorter bond lengths maximize interface effects and make it easier to determine D_s. All our specimens used $l = 25$ mm. We tried longer bond lengths and the results were less reliable. We tried shorter bond lengths, but specimen preparation and handling was difficult. The curve in Fig. 3 shows that specimens with $l = 25$ will have large changes in k

Table 1: Average axial modulus of normal and VTC hybrid poplar strands

Strand	E_L (GPa)
Hybrid Poplar	8.8 ± 0.7
VTC Hybrid Poplar	23.4 ± 1.7

provided D_s is around 5 MPa/mm or higher (or $1/D_s$ is 0.2 mm/MPa or lower). Future development might improve these experiments for greater accuracy at higher D_s by specimen methods that can reliably handle shorter bond lengths.

3. Results

In a DLS specimen, calculation of interfacial properties depends on moduli (E_{Li}) of the strands. Thus, the modulus of each individual strand was measured prior to gluing them together. The average and standard deviations for tensile moduli of hybrid poplar and densified hybrid poplar (VTC) are given in Table 1. The increase in modulus for the VTC strands was roughly proportional to the increase in density by the VTC process (Kutnar, Kamke, Nairn, and Sernek, 2008). Analysis of DLS experiments used the specific moduli for individual strands in each specimen and not these average values.

Selected strands with known moduli were then glued to prepare DLS specimens using PF or PVA resin. To ensure symmetry, we cut one strand with known modulus in half and used the two halves for the two outside strands in the DLS specimen. A different strand, also with known modulus, was used for the central strand. The adhesive bond lines were glued as explained above using a 1% stamp, a 25% stamp, or by manual spreading; the manual spreading method is labeled as the 100% glue bond. All specimens were tested for k and the methods described above

Table 2: The adhesive compliance (1/Ds) and stiffness (Ds) properties for PVA or PF resin bonds with hybrid poplar stands and for PF resin with VTC strands for different amounts of resin coverage. The "No." column is the number of specimens tested for each type.

Strands	Adhesive	No.	1/ D_s (mm/MPa)	D_s Range (MPa/mm)
Hybrid Poplar	PVA 1%	17	0.146 ± 0.056	5.0 to 11
	PVA 25%	16	0.0654 ± 0.0183	12 to 21
	PVA 100%	15	0.0369 ± 0.0196	18 to 58
Hybrid Poplar	PF 1%	22	0.0163 ± 0.0141	33 to 460
	PF 25%	22	0.01048 ± 0.00995	49 to 1890
	PF 100%	22	-0.00022 ± 0.00042	5000 to ∞ / -∞ to -1560
VTC Hybrid Poplar	PF 1%	20	0.01177 ± 0.0064	55 to 186
	PF 25%	20	0.0021 ± 0.00343	181 to ∞ / -∞ to -751
	PF 100%	20	-0.00017 ± 0.00032	6600 to ∞ / -∞ to -2040

were used to calculate D_s. Each measured bond line stiffness was an average of at least 15 specimens.

The results for PVA resin at three coverage levels are in Table 2 and Fig. 3. The value for D_s increased significantly as the glue coverage increased from 1% to 100%. Errors in $1/D_s$ and ranges in D_s were estimated as follows. From experimental results for k, we determined 95% confidence limits. The upper and lower limits were then used separately to solve for D_s. These two results were used to define uncertainties in $1/D_s$ and ranges in D_s. The process is illustrated by the dotted lines above and below the dashed experimental average in Fig. 2. When the range in $1/D_s$ spanned zero, the range in D_s had to be described by two ranges bounded by $\pm\infty$.

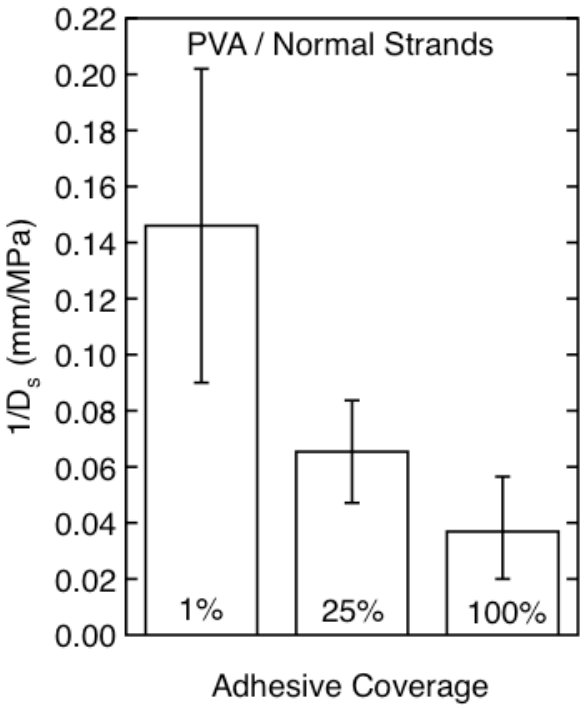

Figure 3: Interfacial compliance ($1/D_s$) as a function of adhesive coverage for normal hybrid poplar strands bonded with PVA resins. The errors bars show the 95% confidence limits in the results.

The results for PF resin on "normal" hybrid poplar strands are shown in Table 2 and on the left side of Fig. 4. As with PVA resin, $1/D_s$ decreased as resin coverage increased, *i.e.*, the stiffness, D_s, of the bonds increased. Compared to PVA bonds, PF bonds were about an order of magnitude stiffer. The $1/D_s$ parameter even became negative for 100% specimens suggesting near perfect bonds and perhaps an effect of penetration reinforcing wood near the bond line. Because of the stiffer bonds, it was difficult to extract the smaller interface effect from the measured global stiffness. This difficulty is reflected in the larger relative error bars for PF experiments compared to PVA experiments.

The results for PF resin on VTC strands are shown in Table 2 and on the right side of Fig. 4. Again, $1/D_s$ decreased as resin coverage increase, *i.e.*, the stiffness, D_s, of the bonds increased. The adhesive stiffnesses for PF/VTC strand specimens were similar to, but slightly higher than the corresponding PF/normal strand specimens. Figure 5 shows SEM images for bonds with normal strands and VTC strands. The normal strands show adhesive penetration into the wood, especially into pores near the bond line. In contrast, the VTC specimen shows virtually no penetration; the densified wood blocks the resin penetration. Despite lack of penetration, the

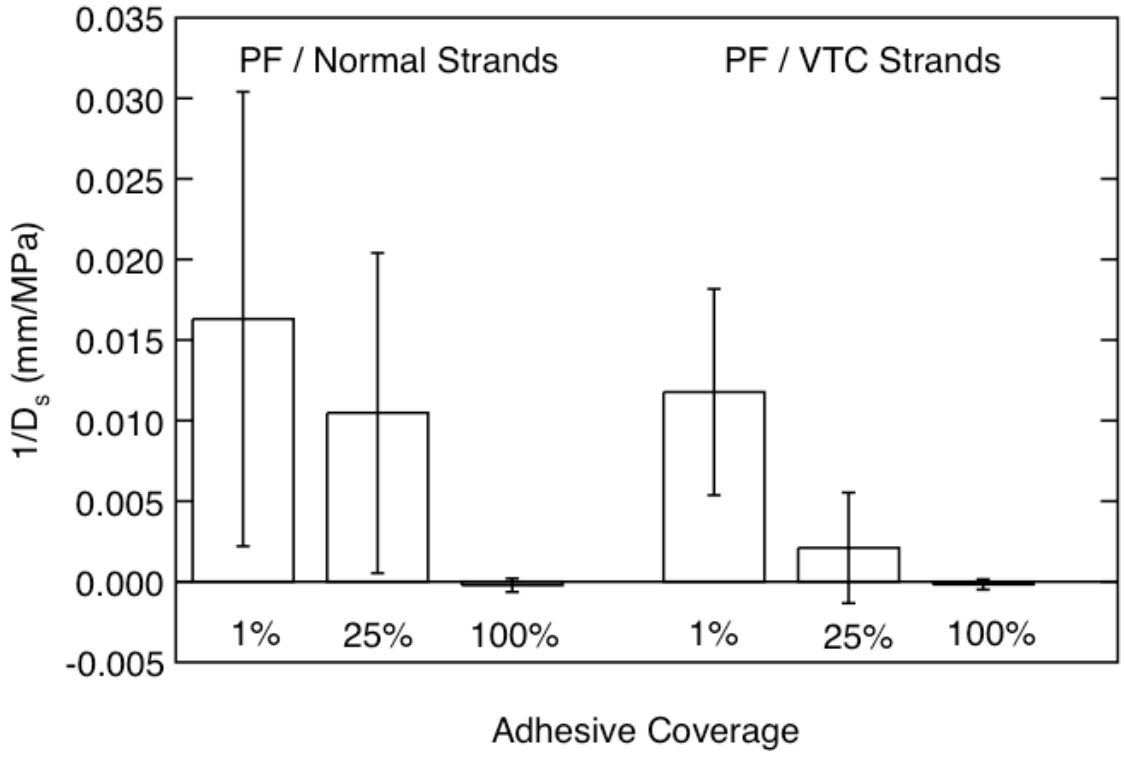

Figure 4: Interfacial compliance ($1/D_s$) as a function of adhesive coverage for strands bonded with PF resin. The left half shows bonding of normal hybrid poplar strands. The right half shows bonding of VTC strands. The errors bars show the 95% confidence limits in the results.

stiffness of the bonds with VTC strands was as high or higher than bonds with normal strands and much greater penetration.

4. Discussion and Conclusions

The new experimental method worked and was able to characterize the stiffness of adhesive bond lines between wood strands. The results always correlated with the amount of adhesive. The extraction of adhesive properties from global results is a challenge. It worked better for PVA specimens because the bonds lines were less stiff and therefore played a larger role in the specimen stiffness. The procedure must rely on well-characterized specimens and well-chosen specimen dimensions. For characterization, it was crucial to measure modulus of each individual strand. If average moduli were used instead, it would have been impossible to extract interface properties. Specimen dimensions also influence scatter in D_s. Future work might be able to reduce uncertainties by developing methods for working with smaller specimens or using experimental techniques for greater accuracy in measuring k.

PVA resin clearly gives much more compliant bonds than PF resin. Even when covered by 100% resin (by manual application), PVA bond lines have measurable compliance that is higher

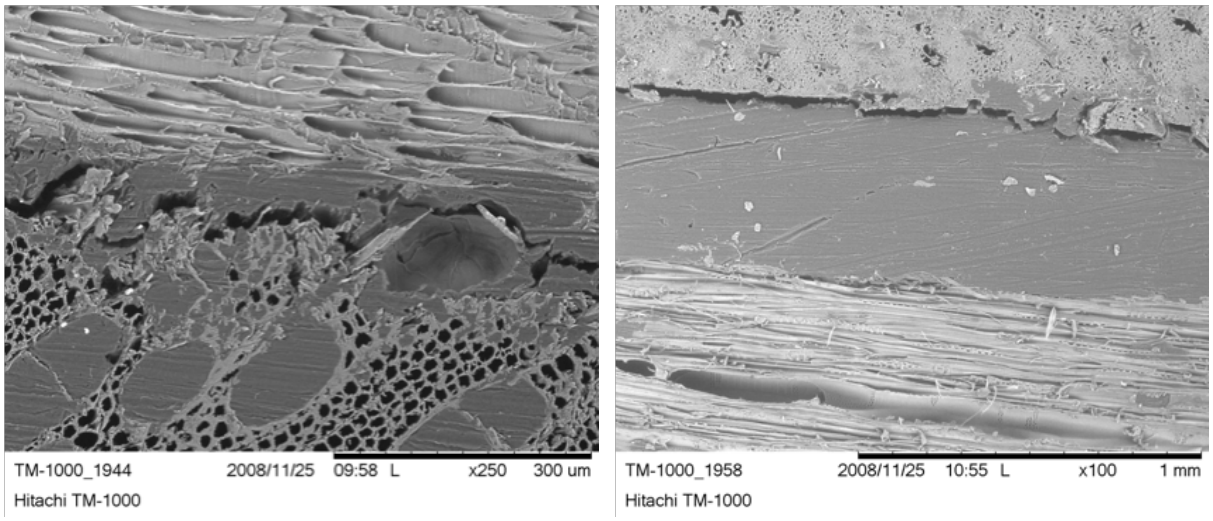

Figure 5: SEM images for 100% coverage bonding of normal hybrid poplar strands (left) and VTC strands (right). Scale bars within the figures indicate magnifications.

than even the lowest coverage PF specimens. Note that the order of magnitude difference in bond line stiffness between PF and PVA is much larger than the stiffness difference between the pure adhesives (López-Suevos 2010). In other words, this testing method is measuring an *in situ* property relating to bond quality that is more than just shear stiffness of the resin.

Although PF bond lines are much stiffer, they still depend on amount of resin coverage. With 100% coverage (manual spreading), the bond line is nearly perfect — $1/D_s$ close to zero. The relevance of this bond line stiffness to wood-based composites, such as OSB made with PF resin, will depend on the amount of coverage seen on actual strands within OSB panels. The ultimate OSB would have all strands with 100% coverage. Such products should have optimal panel properties, but obviously hand application of resin to each strand is impractical. The questions that remain are what is adhesive coverage for typical strands in OSB processing and what are the consequences of less than 100% coverage on OSB properties? The first question could be answered by bond line stiffness experiments for strands coated by OSB resin blender methods. Here the challenge would be to know the mechanical properties of each strand prior to adhesive coverage. The second question could be answered by simulation. We have undertaken that work and some results will be a in a future publication. The results show that $1/D_s$ values in the range observed by these experiments can reduce panel modulus by 10% to 20% (Nairn and Le 2009).

Finally, adhesive bond line experiments may help explain the role of adhesive penetration on the performance of adhesive bonding in wood. These first results suggest penetration has no effect and may even be detrimental to stress transfer. Our experiments for PF/VTC strands, which had no penetration, were always slightly stiffer than experiments for PF/normal strands, which had significant amounts of penetration. But this comparison is not ideal. Although we

varied the amount of penetration, we also changed properties of the strands being bonding. The preferred experiment would be test bond lines between identical strands all with the identical amount of adhesive coverage, but with different amounts of penetration. Unfortunately achieving this ideal is difficult in practice.

5. Acknowledgement

This work was supported by the National Research Initiative of the United States Department of Agriculture (USDA) Cooperative Research, Education and Extension Service, Grant #2006-35504-17444. We also thank Prof. Greg Smith (UBC) for advice on adhesive application methods.

6. References

ASTM (2005) Standard Test Method for Fracture strength in Cleavage of Adhesives in Bonded Metal Joints. ASTM Designation: E 3433.

ASTM (2006) Standard Test Method for Plane-Strain Fracture Toughness of Metallic Material. ASTM Designation: E399-05.

ASTM (2008a) Standard Test Methods for Strength Properties of Adhesive in Two-Ply Wood Construction in Shear by Tension Loading. ASTM Designation: D 2339.

ASTM (2008b) Standard Test Methods for Small Clear Specimens of Timber. ASTM Designation: D 143.

ASTM (2008c) Standard Test Methods for Evaluating Properties of Wood Base Fiber and Particle Panel Materials. ASTM Designation: D 1037.

ASTM (2008d) Standard Test Method for Strength Properties of Double Lap Shear Adhesive Joints by Tension Loading. ASTM Designation: D 3528.

Hashin Z (1990) Thermoelastic properties of fiber composites with imperfect interface. *Mech. of Materials*. **8**: 333–348.

Kutnar A, Kamke FA, Nairn JA, Sernek M (2008) Mode II Fracture Behavior of Bonded Viscoelastic Thermal Compressed Wood. *Wood and Fiber Science* **40**:362-373.

Kutnar, F. A. Kamke and M. Sernek "Densify profile and morphology of viscoelastic thermal compressed wood." *Wood Sci Technol*, **43**, 57-68 (2008)

López-Suevos, F, Eyholzer C, Bordeanu N, and Richter K (2010) DMA Analysis and Wood Bonding of PVAc Latex Reinforced with Cellulose Nanofibrils. *Cellulose* **17**:387–398.

Nairn JA (2004) Generalized Shear-Lag Analysis Including Imperfect Interfaces. *Advanced Composite Letters*. **13**:263-27.

Nairn JA (2007) Numerical Implementation of Imperfect Interfaces. *Computational Materials Science*. **40**:525-536.

Nairn JA, Le E (2009) Numerical Modeling and Experiments on the Role of Strand-to-Strand Interface Quality on the Properties of Oriented Strand Board. *Proc of 9th Int. Conf. on Wood Adhesives*, Lake Tahoe, Neveda, USA, Sept. 28-30.

Smith G (2003a) The lap-shear strength of droplet arrays of a PF-resin on OSB strands. *Forest Prod. J.* **53**:1-7.

Smith G (2003b) A laboratory technique for coating strands with resin droplets of controlled size and spacing. *Forest Prod. J.* **53**:70-76A.